Chapter 9
Shock Response of LPBF Beams with Pockets of Trapped Powder

R Thayne Wagner, Mason Rollans, Matthew S. Allen, and Jeffrey R. Hill

Abstract Laser powder bed fusion (LPBF) is a widely used additive manufacturing technique for producing a variety of components. A common challenge in this process is designing parts that allow unfused powder to be evacuated from internal cavities. However, LPBF can also be leveraged to enhance damping in structures subjected to harsh mechanical environments by intentionally retaining unfused powder within internal cavities. This retained powder enables particle damping, which can reduce resonant vibrations and mechanical shock—offering protection to sensitive electronic components. While several recent papers have explored the frequency response or modal behavior of powder-filled components, there is comparatively less literature on their transient shock response. Understanding the behavior of these components in shock environments can provide insights into damage mitigation that frequency-domain analysis alone cannot offer. The industry standard for transient shock analysis involves comparing shock response spectra (SRS) curves. In this study, we compare the shock responses of powder-filled and monolithic beams using SRS analysis. We investigated their behavior under various impact conditions, measuring input forces with force sensors and structural responses with accelerometers. Results show that, compared to a monolithic beam, beams with unfused powder reduce maximum absolute acceleration by up to 28%.

Keywords Laser powder bed fusion · Impact · Transient response · SRS · Particle damping

Introduction

Additive manufacturing has become an increasingly prominent method for producing complex components. Unlike traditional processes, it enables single-piece designs with intricate geometries, eliminating the need for assemblies of smaller parts [1]. Laser powder bed fusion (LPBF) is a widely used metal additive manufacturing process that fuses fine metal powders layer by layer. However, one challenge is that cavities in a part inevitably trap unfused powder unless provisions are made for draining or post-processing. A second drawback is reduced structural damping. In most assemblies, damping is dominated by joints [2]; eliminating these joints reduces the system's inherent damping. Because damping mitigates vibration-induced damage and noise [3], its reduction can compromise structural performance. Interestingly, these two issues—powder entrapment and reduced damping—can counteract one another when exploited strategically [4, 5, 6, 7, 8, 9, 10].

By embedding unfused powder within LPBF beams, damping can be substantially increased. These pockets function similarly to particle dampers: they dissipate vibrational energy through friction and wall interactions. Prior work has primarily examined the modal behavior of such beams, demonstrating their effectiveness. However, there is limited research on their transient shock response. While particle damping has shown promise in impact-excited beams [11], most prior studies used external filler materials such as plastic beads or tiles [12]. Although effective, such methods introduce additional manufacturing steps and complexity. By instead utilizing the unfused powder inherent to the LPBF process, manufacturing is simplified. The objective of this work is to compare the shock response of a monolithic LPBF beam with that of an LPBF beam containing unfused powder.

R Thayne Wagner · Mason Rollans
Students, Brigham Young University, Department of Mechanical Engineering
e-mail: rtwagner@byu.edu; mrollans@byu.edu

Matthew S. Allen · Jeffrey R. Hill
Professors, Brigham Young University, Department of Mechanical Engineering
e-mail: matt.allen@byu.edu; jeff.hill@byu.edu

© The Author(s), under exclusive license to River Publishers 2026

Kristin B. Zimmerman, PhD (eds.), *Structural Health Monitoring, Metamaterials, Metastructures and Additive Manufacturing and Dynamics of Biomedical and Bioinspired Systems, 2026, Vol. 10*, Conference Proceedings
of the Society for Experimental Mechanics Series, https://doi.org/10.13052/rp-9788743814214

The SRS is a fundamental tool in shock analysis [13]. Typically, acceleration data from a test environment are transformed into an SRS curve. A non-destructive test article can then be excited with inputs of similar frequency content, and its acceleration data converted into an SRS for comparison. If the test article withstands shocks with an SRS equal to or greater than that of the environment, it is deemed suitable. In this study, rather than rating the beams against a specific environment, we subjected a monolithic beam to impact, and then subjected the beam with powder to similar impacts and compared its SRS to the monolithic beam to evaluate peak accelerations.

Methods

Two rectangular 316L stainless steel beams were used, shown in Figure 1. Fabrication details are provided in [4, 5]. One beam was monolithic with no unfused powder, while the other contained a 140mmx16mmx500 μm cavity filled with particles with a mean size of 25 μm. Both beams were identical in overall dimensions. The specimens were subjected to multiple impacts from two modal hammers and a portable pneumatic projectile launcher. Acceleration data were collected and processed into SRS curves for comparison.

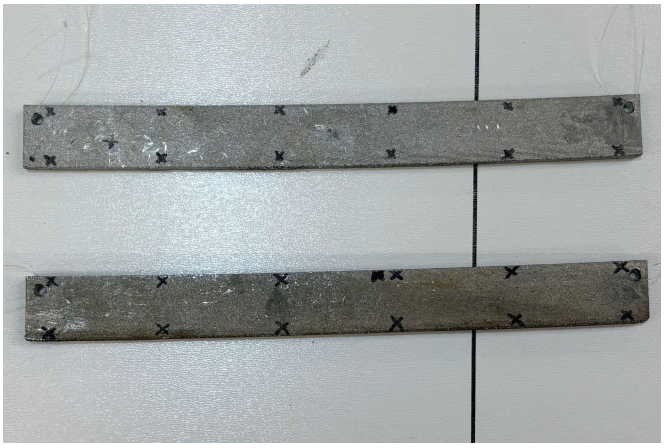


Fig. 1 316L stainless steel beams fabricated by LPBF: powder-filled beam (top) and monolithic beam (bottom). Impact location markers are indicated with black X's.

Hammer Hits

Two hammers were used: a PCB 086D05 modal hammer and an NV-TECH Scalable Automatic Modal Hammer (SAM1). Both were fitted with metal tips to produce short impulses and higher frequency excitation. A PCB 352A21 accelerometer was mounted on the back, left edge of the beam. The beams were suspended by fishing line and bungee cords to approximate free–free boundary conditions, as shown in Figure 2. Each hammer impacted the second marked location from the right end of the beam on the same side as the accelerometer. Accelerometer data were collected at a sampling frequency of 1280 kHz with 20,480 total samples. Five tests were performed for each beam and hammer type. Acceleration was averaged and used to construct SRS curves. Force data were collected and plotted, but used only for reference and not to calculate the SRS.

Portable Pneumatic Projectile Launcher

High-frequency excitation was achieved using a Daisy Powerline 880 portable pneumatic projectile launcher with 4.5 mm diameter (.177 cal) zinc-plated steel shot. The test configuration is shown in Figure 3. The launcher can be seen on the right in each picture and the sample on the far left, with the striker resting on it. Beams were again suspended for free–free conditions. Because direct impacts risked damaging the beams, a striker plate was used. The striker plate measured $4\frac{1}{8} \times 4 \times \frac{1}{8}$ in, and was fabricated from steel. A 1/4 in diameter, 1/8 in thick cylindrical brass bar stock was brazed to the rear of the plate to distribute pressure and soften the impact. The striker plate was suspended in front of the beam so that the brass element just contacted the second marked location from the right end of the beam. A DYTRAN 3224A4 accelerometer was mounted opposite the impact site.

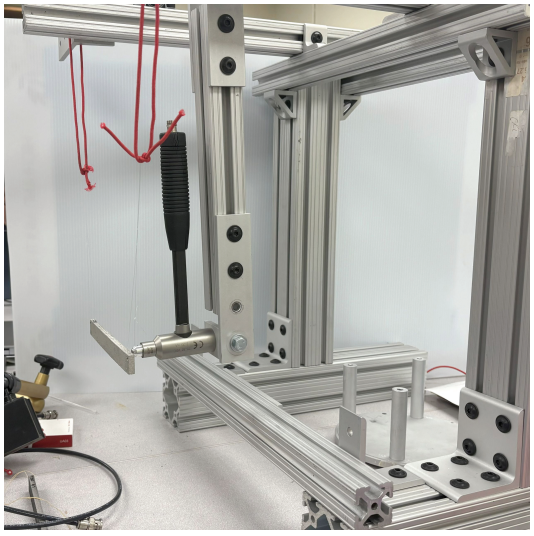


Fig. 2 Experimental setup with beam suspended by fishing line and bungee cords to approximate free–free boundary conditions. A pendulum-mounted modal hammer provided consistent impacts.



(a) Pre-impact (b) Post-impact ricochet

Fig. 3 High-speed video frames of projectile impact on striker plate: (a) initial contact and (b) ricochet. Frame analysis was used to determine projectile velocity before and after impact.

Projectile velocity was measured using a Phantom v1610 high-speed camera. Videos were recorded at 10,000 fps. From these, pre- and post-impact velocities were determined. An additional video at 130,000 fps captured the impact duration. SRS curves were then generated for both monolithic and unfused powder beams.

Results and Discussion

SRS curves were generated using a modified Matlab SRS program. The original program was found at [14]. A damping ratio of 0.002 was used. Acceleration data were captured for both beam cases and used to generate the SRS. Average acceleration data for the SAM1 hammer test are shown in Figure 4 for reference. The acceleration data for the hammers were averaged over the 5 tests, then inputted into the SRS program.

Hammer Tests

Figures 5 and 6 present the SRS results for the SAM1 and PCB hammers, respectively. Five acceleration samples for each case were averaged and normalized by impact force. The trigger for the data collection allowed the data to be synchronized and no correction was needed. This normalization allowed direct comparison of maximum absolute accelerations at the 900 Hz peak. The overall shapes of the SRS curves matched closely between beams, indicating consistent impacts.

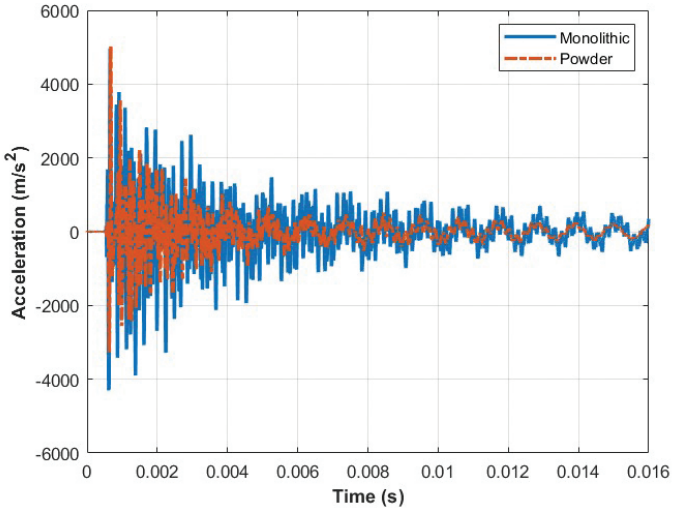
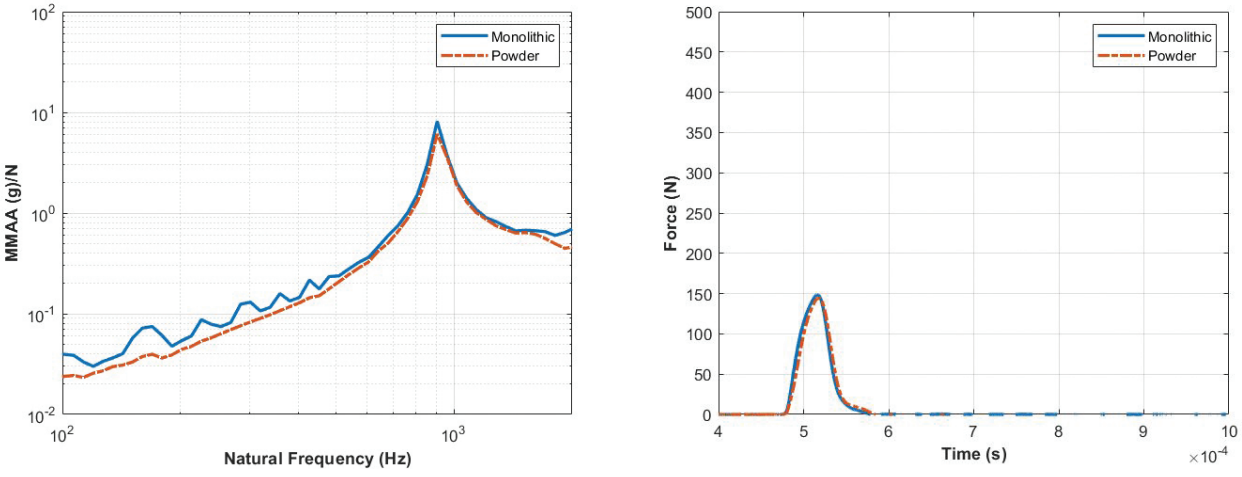


Fig. 4 Average acceleration for the SAM1 hammer of the monolithic beam and the unfused powder beam.

For the SAM1 hammer, the monolithic beam produced a normalized peak of 8.15 g/N, compared to 6.10 g/N for the powder beam—a 28.8% reduction. For the PCB hammer, the monolithic beam produced 14.0 g/N, compared to 13.1 g/N for the powder beam—a 6.6% reduction. In both cases, unfused powder effectively reduced peak acceleration.



(a) SAM1 SRS

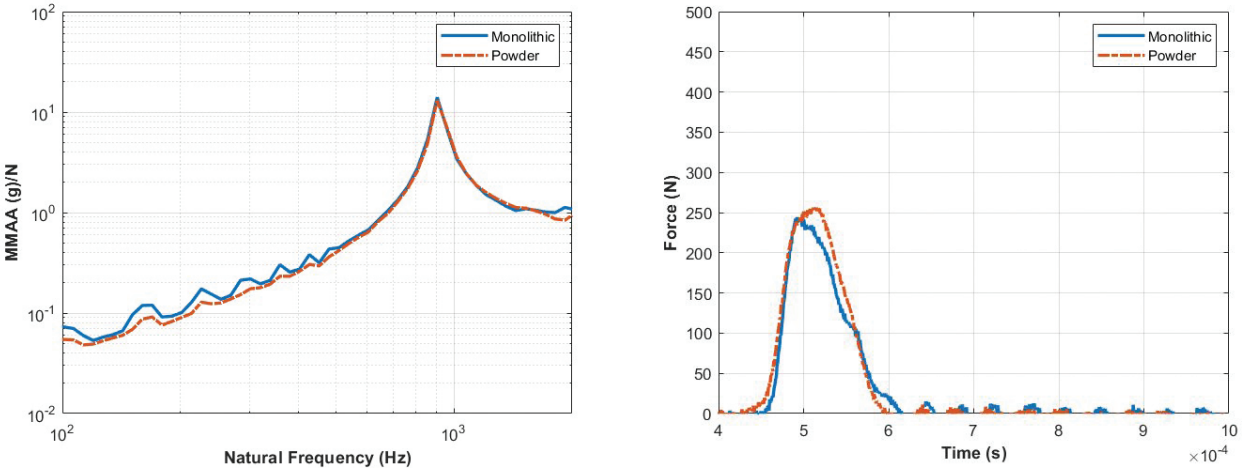
(b) SAM1 Force

Fig. 5 SRS of NV-TECH SAM1 hammer tests. (a) Maximum absolute acceleration normalized by average force. Monolithic peak: 8.15 g/N; powder peak: 6.10 g/N. (b) Averaged force values for monolithic (148 N) and powder (144 N) beams. Data was collected over 16 ms, but was trimmed for the force plot to highlight it's peak force.

Portable Pneumatic Projectile Launcher Tests

Projectile velocities averaged 190 m/s (pre-impact) and 12 m/s (post-impact). Variation across trials was less than 5%, justifying use of average values.

SRS curves for steel shot impacts are shown in Figure 7. Unlike the hammer tests, results were inconsistent. This discrepancy likely arose from test variability. Since the portable pneumatic projectile launcher required manual repositioning between shots, small changes in firing trajectory and striker plate alignment produced non-uniform impacts. The pendulum-mounted striker plate further contributed to variability.



(a) PCB Modal SRS

(b) PCB Modal Force

Fig. 6 SRS of PCB 086D05 hammer tests. (a) Maximum absolute acceleration normalized by average force. Monolithic peak: 14.0 g/N; powder peak: 13.1 g/N. (b) Averaged force values for monolithic (244 N) and powder (251 N) beams. Data was collected over 16 ms, but was trimmed for the force plot to highlight it's peak force.

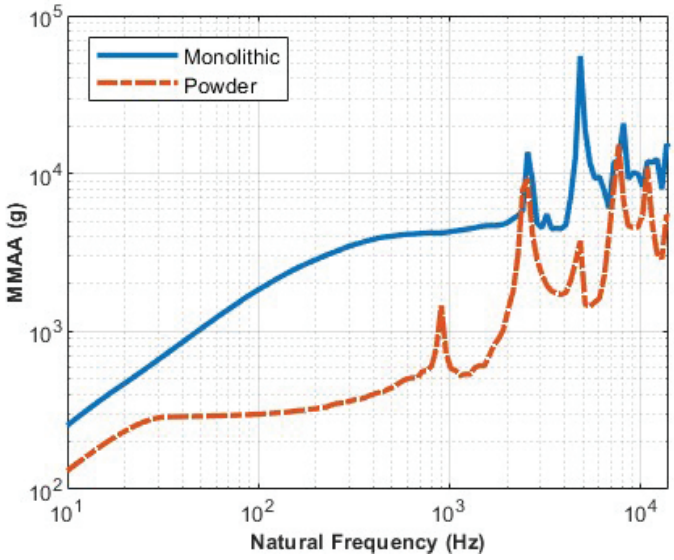


Fig. 7 SRS of beams impacted by steel shot. Monolithic and powder SRS shapes do not match, indicating inconsistent impacts and limiting comparability.

To improve consistency, future tests should employ a gas gun with a tuned resonator plate, as developed in [15]. This method provides a repeatable projectile impact with controlled frequency input, yielding more reliable high-frequency response data.

Conclusions

Unfused powder in LPBF beams effectively increased damping, as evidenced by reduced maximum absolute accelerations compared to monolithic beams under hammer excitation. These results suggest that incorporating unfused powder can reduce structural damage or protect mounted components in dynamic environments.

However, high-frequency tests using a portable pneumatic projectile launcher yielded inconsistent results, highlighting the need for improved impact methods. Future work will employ a gas gun with a resonant plate to provide controlled, repeatable excitation. Additionally, optimization of unfused powder pocket geometries and internal infill structures could further enhance damping performance for specific applications and impact conditions.

References

1. Diegel, O., Nordin, A., and Motte, D. *A practical guide to design for additive manufacturing*. Springer, (2019).
2. Ungar, E. "The status of engineering knowledge concerning the damping of built-up structures". *Journal of sound and vibration*, 26(1):141–154, (1973).
3. Hammami, C., Balmes, E., and Guskov, M. "Numerical design and test on an assembled structure of a bolted joint with viscoelastic damping". *Mechanical Systems and Signal Processing*, 70:714–724, (2016).
4. Teng, S.H. "Investigating the effects of unfused powder damping in laser powder bed fusion". Master's thesis, Brigham Young University, (2023).
5. Black, J.K., Teng, S., Capito, J., Allen, M.S., Nelson, T., and Crane, N. "Damping behavior of trapped powder in additively manufactured steel beams". In *Proceedings of the 42nd International Modal Analysis Conference (IMAC)*, Orlando, FL, USA, (2024).
6. Black, J.K., Andrus, B., Koski, D., Crane, N., Nelson, T., and Allen, M.S. "Nonlinear behavior of additively manufactured steel beams with trapped powder dampers". *Journal of Structural Dynamics*, (Revised Aug. 2025), (2025). available: https://doi.org/10.5281/zenodo.15001945.
7. Schmitz, T., Betters, E., and West, J. "Increased damping through captured powder in additive manufacturing". *Manufacturing Letters*, 25:1–5, (2020).
8. Goldin, A., Scott-Emuakpor, O., George, T., Runyon, B., and Cobb, R. "Structural dynamic and inherent damping characterization of additively manufactured airfoil components". *Journal of Engineering for Gas Turbines and Power*, 143(5):051022, (2021).
9. Ehlers, T. and Lachmayer, R. "Design of particle dampers for laser powder bed fusion". *Applied Sciences*, 12(4):2237, (2022).
10. Scott-Emuakpor, O., George, T., Runyon, B., Holycross, C., Langley, B., Sheridan, L., O'Hara, R., Johnson, P., and Beck, J. "Investigating damping performance of laser powder bed fused components with unique internal structures". In *Turbo Expo: Power for Land, Sea, and Air*, volume 51159, page V07CT35A020. American Society of Mechanical Engineers, (2018).
11. Salvino, L.W., Dupont, P., and McDaniel, J.G. "Evaluation of granular-fill damping in a shock-loaded box beam". In *Proceedings of the 69th Shock and Vibration Symposium*, pages 1–10, (1998).
12. Hill, J.R., Chen, A., Wilson, N., Boll, C., O'Bannon, M., and Trentman, D. "Microbead encapsulation for protection of electronic components". *Journal of Electronic Packaging*, 147(021007), (2024).
13. Sisemore, C. and Babuška, V. *The science and engineering of mechanical shock*. Springer, (2020).
14. Vibrationdata. "Shock & vibration software (srs program)". https://www.vibrationdata.com/software.htm. Accessed: 2025-09-30.
15. Kim, B.S. and Lee, J. "Development of impact test device for pyroshock simulation using impact analysis". *Aerospace*, 9(8):407, (2022).